



## Galactic and Extragalactic Novae - A Review

---

**Rosa Poggiani\***

*Università di Pisa and Istituto Nazionale di Fisica Nucleare, Sezione di Pisa*

*E-mail:* [rosa.poggiani@df.unipi.it](mailto:rosa.poggiani@df.unipi.it)

The outbursts of classical novae are among the strongest explosions in the Universe. The multifrequency observations are contributing to understanding the process of explosions and of the long term evolution. In this review, I discuss the observations of novae over the electromagnetic spectrum, focusing on the morphology of the decline light curves, the spectroscopic investigations, the long term evolution, the recurrent novae, the gamma ray emission in novae, extragalactic novae and the gravitational emission of novae.

*Accretion Processes in Cosmic Sources - APCS2016 -  
5-10 September 2016,  
Saint Petersburg, Russia*

---

\*Speaker.

## 1. Introduction

Classical novae are cataclysmic variable systems in which a main sequence, or evolved star, transfers mass to a white dwarf [78], [19], [15]. The eruptions are caused by a ThermoNuclear Runaway (TNR) on the surface of the white dwarf [19], [15]. The signature of a nova event is the sudden increase in luminosity: novae can achieve an absolute magnitude at maximum in the range from -7 to -10. Even if novae have been observed for centuries, systematic observations started only during the Eighteenth Century [40]. The present optical facilities provide high cadence photometric and spectroscopic observations that contribute to the building of a multiwavelength picture of the nova process together with high energy and radio observations [42]. Classical novae are being investigated over the whole electromagnetic spectrum, from radio to gamma rays. In this paper, I review some aspects of the phenomenology of novae in the context of multiwavelength observations: the morphology of decline curves, the features of the spectroscopic evolution, the Maximum Magnitude Rate of Decline (MMRD) relation, the existence of a sample of faint and fast novae, the nova rates in our Galaxy and in other galaxies, the discovery of high energy emission of novae in the gamma domain. A general introduction to the topics related to novae and cataclysmic variables has been presented by [42].

## 2. Galactic novae

I will firstly discuss some general characteristics of the galactic nova population to provide the context for discussion. The galactic novae have been initially cataloged by [38] and, more recently by [91], [37], [92]. A list of the most recent novae is being maintained by [68]. To date, about 400 novae have been observed in our Galaxy. The sample of Galactic novae has been recently discussed by [108], with a focus on the nova rate, a key parameter in the context of the chemical evolution of the Galaxy. Novae contribute to the chemical evolution of the Galaxy with  $^{22}\text{Na}$ ,  $^{26}\text{Al}$ ,  $^7\text{Li}$ ,  $^{15}\text{N}$ . Some novae, especially recurrent novae, may be the progenitors of type Ia supernovae [107]. The rate of Galactic novae is still uncertain [108], with estimations spanning a wide range. The investigation by [108] found that novae are concentrated in the Galactic plane and towards the galactic center. A revised nova rate has been estimated as  $50_{-23}^{+31}$  per year [108]. The estimates of the galactic nova rate reported in literature are summarized here in Table 1.

The distribution of orbital periods shorter than 10 hours (that is, mostly with non-evolved secondaries) is reported in Fig. 1. The distribution has been built using the catalog by [91], [92]. The majority of novae have orbital periods above the period gap of cataclysmic variables, with a peak between 3 and 4 hours, unlike other cataclysmic variables [123]. The population of novae is also dominated by systems with an high mass accretion rate [123].

The light curve decay is the signature of a nova event. The rise to maximum is generally fast and is followed by a decline, whose characteristic time determines the speed class of the nova. The time scale of the decline is related to the magnitude at maximum: brighter novae show a faster decline. The light curve during the decline is the basis of the standard method to estimate the distance of novae, the Maximum Magnitude Rate of Decline (MMRD) relationship, that has been investigated by several authors using samples of Galactic and extragalactic novae [98], [28], [23], [34], [36]. The dominant parameter in the MMRD relations is the mass of the underlying

Authors	Rate (yr <sup>-1</sup> )
Allen 1954 [7]	100
Sharov 1972 [115]	260
Liller and Mayer 1987 [57]	73±24
Della Valle 1988 [29]	15±5
Ciardullo et al. 1990 [21]	11 to 46
van den Bergh 1991 [126]	16
Della Valle and Livio 1994 [33]	20
Shafter 1997 [100]	35±11
Hatano et al. 1997 [46]	41±20
Shafter 2002 [101]	36±13
Matteucci et al. 2003 [60]	25
Mroz et al. 2015 [65]	13.8±2.6
Shafter 2017 [108]	50 <sup>+31</sup> <sub>-23</sub>

**Table 1:** Estimation of the galactic nova rate reported in literature

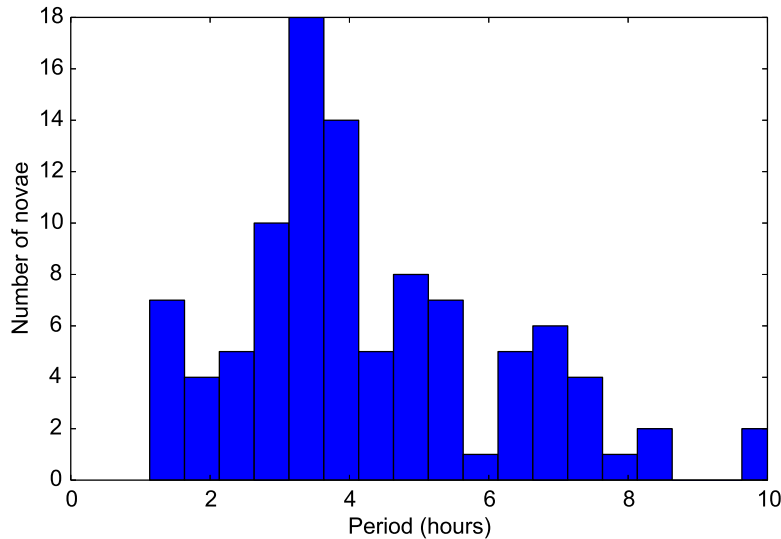


**Figure 1:** Distribution of orbital periods of galactic novae; data from [92]

white dwarf [59], brighter and faster novae have more massive dwarfs. The simulations by [136] predicted that some classical novae could deviate from the MMRD relation. Samples of faint and fast extragalactic novae with a strong scatter around the MMRD relation have been observed in M31 by [55] and in M87 by [113]. The large scatter suggests that the extragalactic novae cannot be used as standard candles [114]. The faint and fast novae are systems that have accreted very low mass envelopes on massive white dwarfs and include recurrent novae [114]. A new estimation method for the distance of galactic novae has been presented by [75]. The method is based on the location of the red clump giants in infrared color-magnitude diagrams. Reddening-distance relations have been derived and combined with independent reddening estimates. The approach has been calibrated with the novae with shells for which the expansion parallax has been measured [36]. The authors have estimated the distance of 73 novae and the lower limit for 46 objects. The

estimated distances are in agreement with the expansion parallax results.

## 2.1 Photometric evolution

The light curve of novae during the decline does not necessarily follow a monotonous brightness decrease, but can exhibit a rich pattern, including oscillations, dips, cusps, flares... [15]. A catalog of 93 light curves and a classification system have been recently suggested by [119]. The authors suggest seven prototype classes, according to the features exhibited during the decline: the F-class novae with flat top; the C-class novae have a cusp; the J-class novae show jitters; the P-class novae show a plateau; the O-class novae show oscillations; the S-class system show a featureless decline; the D-class novae show dips. The different classes account for 2%, 1%, 16%, 21%, 4%, 38%, 18% of all novae, respectively: the expected smooth decline holds for less than one half of novae. A synoptic view of the decline curves, modeled after [119], is reported in Fig. 2.

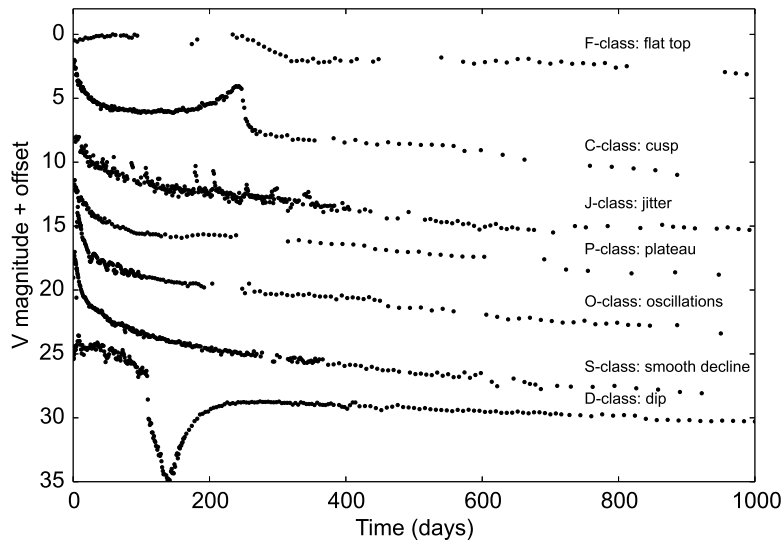


**Figure 2:** The morphological classes of the novae light curves, after [119]; data from [119]

The contribution of citizen astronomers and small telescopes has traditionally played a relevant role in the photometric coverage of the novae evolution: the archives of AAVSO<sup>1</sup> and VSNET<sup>2</sup> are a source of photometric data from the nova discovery to the late decline. The AAVSO activities are described in detail in the contribution presented by [54] to this conference.

Recently, different surveys aiming to monitor sky variability have provided high cadence photometric data of nova eruptions, covering also the pre-maximum stage and investigating the orbital period of the systems. The ground based Optical Gravitational Lensing Experiment (OGLE) has monitored novae in the Galaxy [65] and in the Magellanic clouds [66]. The Galactic survey [65] has monitored 39 novae eruptions, with about one third of the objects discovered by the survey itself, and 80 post-nova candidate systems; in addition, orbital periods were estimated for 18 objects. The space based Solar Mass Ejection Imager (SMEI) is an high cadence instrument, with a

<sup>1</sup><https://www.aavso.org/>

<sup>2</sup><http://ooruri.kusastro.kyoto-u.ac.jp/mailman/listinfo/>

time spacing of about 100 minutes, that has monitored a total number of 13 galactic novae [50], [51]. The high temporal cadence has allowed to investigate the pre-maximum halt stage, seldom covered in detail. Some novae targeted by SMEI were discovered by ground based observatories only weeks after the achievement of the maximum luminosity, suggesting that many classical novae could be overlooked, including bright ones, as discussed also by [108].

The decline curves of novae without oscillations or dust dips have been studied by [44], [56]. A large part of the envelope is ejected by winds, that are accelerated inside the photosphere. After its maximum expansion, the photosphere starts to shrink, while the ejecta are expanding. The optically thin ejecta and the photosphere produce the optical and UV/X-ray radiation. The light curves calculated for a range of masses and compositions of the white dwarf, after rescaling by a suitable time factor follow a universal decline law. The luminosity declines as  $t^{-1.75}$  in the interval from 2 to 6 magnitudes below the optical maximum and as  $t^{-3.5}$  later, in the region from 6 to 10 magnitudes below maximum, where  $t$  is the time elapsed from the outburst in days. The break on the light curve could be caused by the drop in the wind mass loss rate [44]. The universal decline law allows the estimation of the on and off times of super-soft X-ray emission [45]. The two times are  $t_{on} = (10 \pm 1.8)t_3$  and  $t_{off} = (5.3 \pm 1.4)t_3^{1.5}$ , respectively, where  $t_3$  is the intrinsic decay time by three magnitudes in the universal decay curve. The absolute magnitude at 15 days after the optical maximum is almost identical for all novae,  $M_V(15) \sim -5.7 \pm 0.3$ .

## 2.2 Spectroscopic evolution

The novae can be divided into two main spectral classes [130], [131]. Novae in the Fe II class are slow to moderately fast, showing Fe II lines as the strongest non Balmer lines in early stage spectra and auroral and forbidden lines in nebular spectra; the emission mechanism is wind ejection. Novae belonging to He/N class are fast, exhibiting broad He or N lines as the strongest non Balmer lines in the early stages spectral broad lines, replaced by coronal lines in the nebular spectra; the emission mechanism is shell ejection. In the initial classification system, a few novae were classified into the hybrid class, showing a switch from the Fe II class to He/N class; the underlying mechanisms are weak winds and shell ejection. The observations of V5558 Sgr [121] and T Pyx (see e.g. [53], [41]) have shown that novae can also switch from an He/N to a Fe II spectrum. According to [135], the He/N and Fe II spectra suggest an origin in the white dwarf ejecta or in a circumbinary gas envelope whose origin is the secondary star. The contribution of the two mechanisms varies during the decline stage: the majority of novae is expected to show both kinds of spectra during the early evolution [135]. Two distinct nova populations exist in the Milky Way, with fast novae closer to the galactic plane than slow novae [30]. In addition, fast and slow novae belong to the two distinct spectral classes, He/N and Fe II [130], [131], with the former being faster and more luminous [35].

A spectral atlas of mostly Southern novae has been built and is continuously updated by the SMARTS Consortium [128], [129], as the successor of the Tololo nova atlas [132], [133]. As of 2017, the atlas contains more than seventy novae, with optical/IR photometric and spectroscopic data secured with the ANDICAM dual channel imager and the RC spectrograph at the SMARTS 1.5 m telescope [128]. The atlas has allowed several studies [129]. The switching on and off of the super-soft emission have been investigated by coordinating observations with Swift: He II 4686 in fast He novae shows a temporary increase just before the onset of the super-soft phase and a drop

after when it has turned on [129]. The absence of He II 4686 when the Bowen blend is visible is probably caused by a temperature effect [129]. The novae that form dust can show a dip in the decline light curve, a few weeks or months after the outburst. The flux in the  $K_s$  band shows an increase before the beginning of the dip, but it increases also in novae that form dust, but not show dips in the light curve [129].

I am monitoring novae (mostly Northern) since 2005 at the Cassini 1.5m telescope equipped with the BFOSC Imager/Spectrograph [89]. Optical spectra are secured during the decline to monitor the evolution of the novae, with the highest possible cadence. The sample includes more than twenty Galactic novae and some extragalactic novae: V1663 Aql [80], V1722 Aql, V809 Cep, V962 Cep, V2362 Cyg [83], V2467 Cyg [84], V2468 Cyg, V2491 Cyg, V2659 Cyg, V407 Cyg, V339 Del, KT Eri, V959 Mon, V2670 Oph [85], V2944 Oph, V496 Sct, V556 Ser, V5558 Sgr [81], [86], V5584 Sgr [88], V458 Vul [82], V459 Vul [87], M31 2009-10b, M31 2010-07a, M31 2011-07 and M33 2010-07a [90]. The results of the investigation of some novae with a peculiar photometric and spectroscopic behavior are briefly summarized here. V2362 Cyg showed a cusp during the decline and underwent a secondary mass ejection [83]. V2467 Cyg showed oscillations during the decline and an early appearance of forbidden lines [84]. V5558 Sgr is a very slow nova containing a white dwarf with a mass at the lower limit to trigger a nova outburst [81], [86]. V458 Vul is an hybrid nova that switched from the Fe II to the He/N class during the decline [82]. M31 2009-10b was one of the most luminous novae in M31 [90], while M33 2010-07a is the first nova in M33 showing a secondary mass ejection [90].

### 2.3 Long term evolution

The pre-eruption and the long term behavior of novae are still poorly understood, since the photometric and spectroscopic coverage is sporadic before the outburst and becomes sparser after the few months following the outburst, also for recurrent objects. The long term evolution has been discussed by [77].

The pre-eruption light curves of novae have been initially investigated by [93], who suggested that 5 out of 11 objects showed a brightness rise in the years before eruption; most novae showed the same magnitude in quiescence before and after the outburst. A new investigation by [24] showed that the pre-eruption brightness rises were rarer than previously believed, being present only in two out of 22 novae under consideration. The authors confirmed that most novae do not show changes in quiescent magnitude before and after the outburst, with the exception of a few systems, with post eruption brightness larger by one order of magnitude.

A critical point is the possibility of hibernation of novae between eruptions [110], switching to a low mass transfer state. For the majority of novae, mass loss dominates during the outburst, separating the secondary from its Roche lobe and switching off the mass transfer after irradiation. The phase of large mass loss can persist for decades. During the hibernation period, the combination of magnetic braking and gravitational wave emission shrinks the distance of the components until the contact with the Roche lobe is re-established. Old novae are still relatively bright for decades due to the irradiation by the white dwarf. Later, the irradiation decreases and the accretion rate slows down. The hibernation model predicts a cyclical evolution between stages with high and low mass transfer. As the mass transfer rate slows down, the nova begins a stage where dwarf nova outbursts occur and the overall brightness decreases. The hibernation phase can last hundreds thousands or

million years. The hibernation hypothesis is supported by the rate of decline of old novae [39] and the observation of shells around the dwarf novae Z Cam [111] and AT Cnc [112].

Novae in quiescence or post-novae are of paramount interest to understand the physical conditions leading to nova outburst and the modifications of the system after the event. A large effort is going on. The search for old novae is performed using multicolor photometry and spectroscopy [122], [76]. The older novae listed in the catalogs of cataclysmic variables [37] often do not have an identified optical counterpart [122], [76]. The selection of objects is performed using their position on the color-color diagram. The combination of the white dwarf, red dwarf and accretion disk shifts the position away from the main sequence curve [122]. Follow up spectroscopy is used to confirm the photometric classification.

The observations of V1213 Cen secured by [67] from the pre-maximum to the outburst stages have shown the awakening of the object from the hibernation phase. After the 2009 outburst, V1213 Cen underwent a slow decline from 2010 to 2016, with a fading rate of about half a magnitude per year. The pre-eruption data in the interval from 2002 to 2010 show some dwarf nova outbursts with an amplitude of about three magnitudes, lasting for one or two weeks and spaced by two or three weeks, in analogy to the behavior of the U Gem systems. The brightness in quiescence is compatible with the brightness of dwarf novae. The outburst features suggest a low mass transfer rate. The nova eruption of V1213 Cen occurred less than a week after the onset of a dwarf nova outburst. The mass transfer rate after the nova eruption was higher than before the event, as a consequence of the eruption.

## 2.4 Recurrent novae

All novae are believed to be recurrent, but the intervals between outbursts can be as long as tens thousands years. The recurrence time is mostly determined by the mass of the white dwarf and the accretion rate [136]. The recurrent novae are defined as the novae with a recurrence time smaller than one century. These systems are particularly suitable for studying the accretion process, due to their cyclic behavior. Recurrent novae are candidates as progenitors of supernovae type Ia [120]. To date, there are 10 known recurrent novae in the Galaxy [97], 4 in LMC [72] and 12 in M31 [107]. The photometric history of all galactic recurrent novae (for a total of 37 eruptions) has been presented by [97]. An example of the photometric data is shown in Fig. 3 for the 2006 outburst of RS Oph. RS Oph has undergone outbursts in 1898, 1907, 1933, 1945, 1958, 1967, 1985, 2006. The white dwarf in RS Oph is believed to be massive and accreting material at a high rate.

Generally, recurrent novae are fast and belong to the He/N spectral class and have an high rate of mass transfer, to explain the short interval between outbursts [72]. The recurrent novae are classified into three classes. The systems T Pyx, IM Nor and CI Aql have an orbital period smaller than one day and the secondary star that is probably still on the main sequence. The systems U Sco, V394 CrA and V2487 Oph have orbital periods of the order of one day and contain an evolved secondary. The systems T CrB, RS Oph, V745 Sco and V3890 Sgr are symbiotics, with large orbital periods, of the order of years, and a red giant secondary.

## 2.5 High energy emission

The X-ray emission of novae has been presented by [69], [71], [74]. Novae are transient X-ray

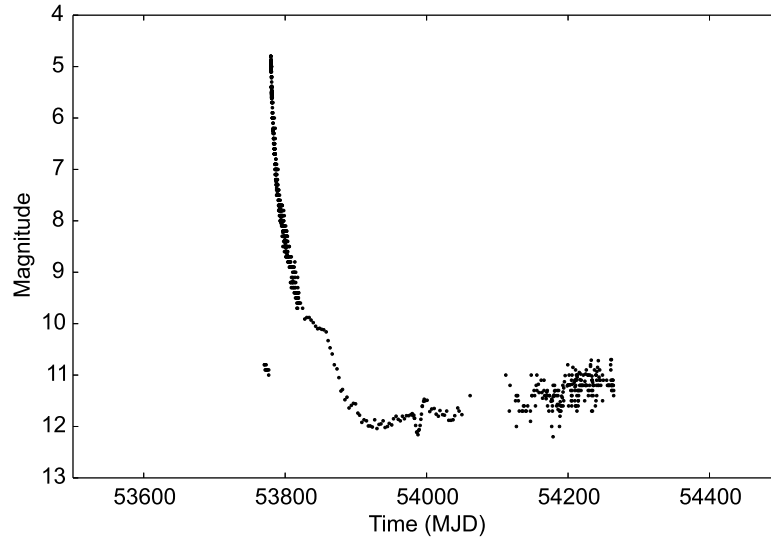


**Figure 3:** The 2006 outburst of RS Oph; data from [97]

sources. The observations of classical novae weeks to months after the outburst show complex X-ray spectra [70]. A relevant part of X-ray emission is coming from the nova shell. In recurrent novae or novae with red giant secondaries the source of emission may be circumstellar matter that has been shocked by the nova wind. For the majority of classical novae the X-rays are produced inside the ejected nebula [70]. The X-ray observations of novae are discussed by [73] in these proceedings and will not be discussed here.

Gamma ray emission in novae was expected in the region of MeV energies, from positron annihilation and nuclear de-excitation following the decays of nitrogen, oxygen and sodium [22]. A summary of gamma ray emission in novae can be found in the paper [48]. Surprisingly, the first detection of gamma rays from a nova was in the GeV energy region. The Fermi-LAT instrument [13] has observed the GeV radiation of the symbiotic nova V407 Cyg in the region 0.1 to 10 GeV [3]. The unexpected emission was explained by the interaction of the material in the nova shell with the environmental medium of the red giant component. The first nova showing high energy emission is a symbiotic system, where ejecta expand inside a relatively dense circumstellar wind, allowing acceleration of particles in a blast wave. The environment around classical novae has a lower density, thus the acceleration can be explained by a bow shock driven by the ejecta in the ISM or by the presence of turbulence and the production of smaller shocks [4]. The Fermi-LAT has detected GeV gamma ray emission in the novae V959 Mon, V1324 Sco and V339 Del [4]. The three classical novae share a common pattern, a soft spectrum that persisted for a few weeks. The finding suggests that all novae are potential gamma ray emitters. The underlying physical processes could depend on properties of the system, such as the mass of the white dwarf or the mass transfer rate. The possible mechanisms considered for gamma ray emission in novae are the hadronic and the leptonic scenarios [4]. In the former scenario, the nova ejecta interact with the nuclei of the environmental medium (or the stellar wind in symbiotics) producing neutral pions that decay to photons. In the latter, the gamma rays are produced by the interaction of accelerated electrons with



photons in the inverse Compton scattering or with atoms via bremsstrahlung.

The Fermi-LAT instrument has observed also the GeV emission of the novae V1369 Cen and V5668 Sgr [20] in the first tens days after the outburst. The gamma radiation was detected as early as two days after the optical maximum and persisted for tens days after the peak. The gamma ray emission was fainter, but showed a longer duration compared to the gamma ray novae described in [4]. The two novae showed peculiar secondary peaks in the optical decline curve during the observations of Fermi-LAT. The count maps of four gamma ray novae observed by Fermi LAT are shown in Fig. 4.

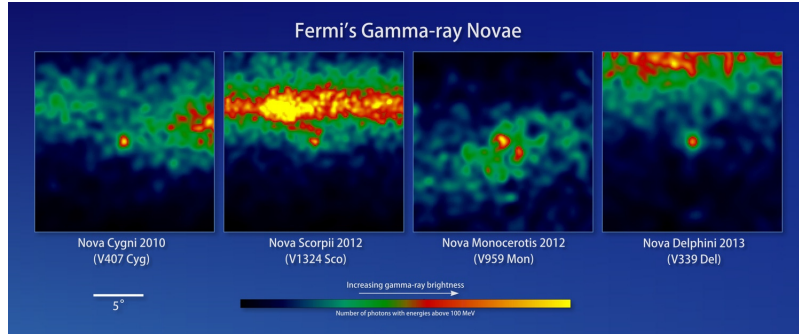


**Figure 4:** Count maps of four new gamma-ray novae observed by Fermi-LAT; adapted from <https://fermi.gsfc.nasa.gov/science/etev/binaries/>

An investigation of the gamma ray emission of non-symbiotic novae and the role of the hadronic and leptonic models has been presented by [62], [63]. The gamma ray emission in novae probes the physical processes related to the relativistic particle acceleration at non relativistic shocks [62]. The shocks are probably radiative, because of the high density of the ejecta at the epoch of emission of gamma rays. The X-rays following the shock are absorbed in the neutral gas and transformed into optical radiation. The gamma rays are the product of the collision of protons with the ejected material (hadronic model) or come from the emission via inverse Compton or bremsstrahlung of relativistic electrons (leptonic model). The fraction of the shock power spent in the acceleration of relativistic particles is determined by the ratio of the gamma ray to optical luminosity, that for the novae V1324 Sco and V339 Del is larger than the value derived from galactic cosmic rays, disproving leptonic models. The fraction of optical luminosity powered by shocks is non negligible. The authors predict the emission of X-ray radiation in the range 10 to 100 keV, in coincidence with GeV emission. The investigations of shocks in novae has been presented by [118] at this conference.

The discovery of gamma ray emission of novae in the range 0.1 to 1 GeV has triggered the investigation of the shocks and the relativistic particle acceleration involved in the outburst [63]. The gas upstream of the shock is neutral and shielded by ionization. The acceleration is confined to a thin photo-ionized layers just ahead of the shock itself. The maximum energy achieved in the acceleration can be as high as 10 GeV to 100 TeV. The high energy radiation can be potentially detected with ground based atmospheric Cherenkov detectors, such as the Cherenkov Telescope Array CTA [5]. The expected TeV neutrinos could be detected by IceCube, at least for close novae, and could bridge multiwavelength investigations of novae with multimessenger astronomy. The

theoretical modeling of gamma and neutrino emission in gamma ray novae has been discussed by [117].

The ground based atmospheric Cherenkov telescope MAGIC has monitored novae and dwarf novae in the region above 50 GeV [6]. If the GeV emission can be explained by the inverse Compton scattering of electrons accelerated in a shock, protons in the same environment could be accelerated at high energies, contributing to the TeV spectrum. The observations of nova V339 Del after its outburst showed no significant TeV emission, but set an upper limit to the emission. The combination of MAGIC and Fermi data of V339 Del showed that the total power of accelerated protons was smaller than the 15% of the total power of accelerated electrons.

### 3. Extragalactic novae

The high luminosity of novae makes them observable in other galaxies, at least the closest ones, circumventing the problem of galactic interstellar reddening and its variation with the direction. Extensive coverage of extragalactic novae is made difficult by the distance of host galaxies. However, the typical magnitudes of novae in M31, M33, LMC at maximum and during the early decline make them suitable candidate targets for medium size telescopes, that in principle can secure frequent observations. The different stellar populations in other galaxies could have an impact on the evolution of their novae and on the nova event rate, thus extragalactic novae are a tool to understand nova populations. Extragalactic novae can show the non standard photometric and/or spectroscopic behaviors sometimes observed in galactic novae: high luminosity, secondary outbursts, oscillations etc. A review of extragalactic novae has been presented by [106].

The rate of novae in galaxies of different types has been addressed by [137] using population-synthesis techniques. The nova rate in a galaxy is governed by the its star formation rate (SFR) history. The nova rate per unit mass, i.e. per unit of K-band luminosity, is higher for low mass galaxies than for high mass ones. The possible difference in disk and bulge novae are explained by the belonging of bulge novae to an older stellar population that leads to less massive white dwarfs. The K-band luminosity specific nova rate is predicted to be lower in elliptical galaxies, where star formation occurred mostly in an initial burst, than in other types of galaxies. Theoretical nova rates in galaxies with different Hubble type have been estimated by [60].

The majority of the statistical investigation of extragalactic novae is coming from the close galaxies M31, M33, LMC, that will be discussed in the following. The catalogs of extragalactic novae are available at <http://www.mpe.mpg.de/~m31novae/opt/> [79]. As of May 2017, the number of known novae in M31, M33, LMC are 1071<sup>3</sup>, 50<sup>4</sup> and 50<sup>5</sup>, respectively.

The identification of novae in M31 and the estimation of rate have been the subject of several investigations. The first surveys by [52] and [12] estimated rates of about 30 novae yr<sup>-1</sup> and 26±4 novae yr<sup>-1</sup>, respectively. New surveys were performed by [94], [95], [96]. The initial surveys had been missing a fraction of novae occurring close to the nucleus, because of the saturation of the photographic plates, and in the outer disk, due to obscuration by dust [17]. Novae in M31 can indeed occur in any part of the galaxy: as discussed by [21] the most part of them is concentrated

<sup>3</sup><http://www.mpe.mpg.de/~m31novae/opt/m31/index.php>

<sup>4</sup><http://www.mpe.mpg.de/~m31novae/opt/m33/index.php>

<sup>5</sup><http://www.mpe.mpg.de/~m31novae/opt/lmc/index.php>

in the bulge and in the halo [17]. According to [17], the estimated nova rate in M31 is  $29 \pm 4 \text{ yr}^{-1}$ . A more recent estimation of a rate of  $37_{-8}^{+12} \text{ yr}^{-1}$  by [109] suggested an higher value. A larger rate,  $65_{-15}^{+16} \text{ yr}^{-1}$  was derived by [26], who suggested the existence of two nova populations, in bulge and in disk. A systematic spectroscopic investigation of the novae in M31 has been performed by [125]. The multiyear spectroscopic survey of novae in M31, including 46 objects, has doubled the number of samples with measured spectra [103]. The fraction of novae belonging to the Fe II and He/N class were 82% and 18%, respectively, in agreement with the population of galactic novae. No relation was found between the spectral class of novae and their position in M31. On the other hand, the spectral class is related to the speed class, as in galactic novae: the brighter novae show a faster decline and belong to the He/N class. The fraction of recurrent novae in M31 is of the order of a few percent [107]. Among them, nova M31 2008-12a is particularly relevant, since it shows the shortest recurrence time,  $175 \pm 11$  days [47]. The nova has been observed during several outbursts; the monitoring of the 2015 outburst is reported by [27]. The high cadence survey of the Palomar Transient Factory (PTF) has monitored the light curves of 29 novae in M31 with a high cadence, from minutes to days [16]; eight novae of the sample have been monitored also in the near-ultraviolet (UV) band with the Galaxy Evolution Explorer (GALEX). Two novae, M31 2009-10b and M31 2010-11a, show UV emission with a peak a few days before the optical maxima. The authors suggest that this could be explained by an aspherical outburst.

The nova rate in M33 is expected to be larger than in M31, since M33 is an early type galaxy [31]. The initial estimates of the rate ranged from less than  $0.4 \text{ yr}^{-1}$  [116] to  $4.7 \pm 1.5 \text{ yr}^{-1}$  [31]. The rate of novae in M33 has been recently estimated as  $2.5_{-0.7}^{+1.0} \text{ yr}^{-1}$  [134]. The authors suggest that, due to the uncertainties in the nova rates, there is no indication of a strong link to the Hubble type of the host galaxy. A spectroscopic survey of novae in M33 has been presented by [104]. The sample contained six novae with spectroscopic classification, that were merged with two other systems with measured spectra. Five out of eight novae belonged to the He/N class, while two of them belonged to the Fe II class. The result marks a difference in M33, compared to the Galaxy and M31, dominated by Fe II novae with a fraction of about 80%. The larger fraction of He/N novae in M33 can be explained by its younger stellar population, that produces novae with more massive white dwarfs than in the Galaxy or M31.

The nova rate in LMC is still under investigation. The rate has been initially estimated by [43] in the range from 2 to 3 novae per year. New rates of  $2 \pm 1 \text{ yr}^{-1}$  [18] and of  $2.5 \pm 0.5 \text{ yr}^{-1}$  [32] were later estimated. The Magellanic survey by the OGLE experiment [66] has recently monitored 20 eruptions of novae in LMC and SMC, one half of them discovered by the survey. The survey estimated a nova rate of  $2.4 \pm 0.8 \text{ yr}^{-1}$  in LMC. The K-band luminosity specific nova rate is higher than in other galaxies, probably due the peculiar star formation history, that underwent a re-ignition. Novae in LMC has been investigated by [105], who secured photometric data for 29 novae and spectroscopic data for 18 objects. The fraction of novae belonging to the Fe II and He/N class is approximately identical, in contrast to the dominance of Fe II novae in the galaxy and in M31, but in agreement with M33 data. The He/N novae show a faster decline, as novae in the Milky Way and in M31, but the decline times are generally shorter. The large fraction of He/N novae in LMC than in the Galaxy is probably due to its stellar population. Being younger, the population of LMC produces nova progenitors containing more massive white dwarfs, that lead to fast He/N novae. An additional consequence is the large number of recurrent novae, about 10%.

The wealth of information that extragalactic novae can provide is demonstrated by the observation of a sample of faint and fast novae [55]. The authors have performed a photometric and spectroscopic follow up of novae in M 31, M 81, M 82, NGC 2403, NGC 891 using the Palomar 60 in telescope. The follow up had an high time cadence, imaging the target galaxies every night. The observed novae did not fit into the standard MMRD relation, being a class of faint but fast classical novae in a yet unexplored region of the luminosity vs. time scale diagram. The process of nova outburst is determined not only by the mass of the white dwarf [59], but also by other variables, such as the composition, the temperature, the accretion rate [55]. The faint and fast novae could be produced by massive and hot white dwarfs [55], as predicted by [136].

On the other end of the brightness, some extragalactic novae have been superluminous. The objects LMC 1991 [99], SN 2010U in NGC 4214 [25], M31 2007-11d [102], M31 2009-10b [90] are, surprisingly, all Fe II novae, in contrast to the higher luminosity expected in He/N novae. The simple correspondence between Fe II novae and older stellar populations with less massive white dwarfs does not necessarily hold; probably the superluminous novae are systems with cool dwarfs accreting material at a very slow pace [25]. The photometric evolution of the four luminous novae and the spectrum of M31 2009-10b showing Fe II lines are reported in Fig. 5.

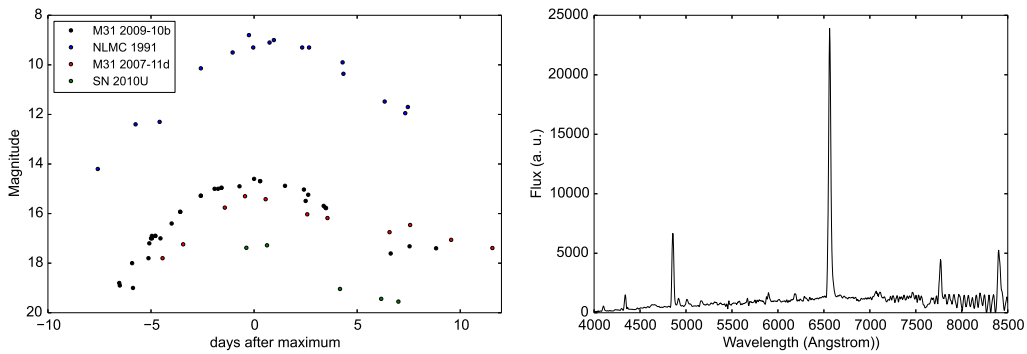


**Figure 5:** Left: light curves of the superluminous novae M31 2009-10b (R band), LMC 1991 (V band), M31 2007-11d (unfiltered, minus three magnitudes), SN 2010U (R Band), see [90] and references therein. Right: spectrum of M31 2009-10b secured by [90] on 2015 October 25

#### 4. Novae as possible gravitational wave emitters

The recent first direct detection of gravitational waves by the Advanced LIGO interferometers of the black hole merger GW150914 [1], later confirmed by a second event, GW151226 [2] has opened a new observational window in astronomy. Novae, and cataclysmic variables in general, are candidate emitters of gravitational waves in the sub-Hz region, that includes a large variety of other sources, from compact binaries to massive black hole binaries to stellar mass black holes inspiraling onto supermassive black holes [64]. The frequency region below one Hz is not accessible by ground based interferometers, due to the seismic noise. It is necessary to use laser interferometers operating in space [127]. An additional advantage is the possibility to achieve very long arm lengths.

The first conceptual study of the space based interferometer LISA was performed by NASA and ESA [58]. The basic principle of the measurement is sensing of the tidal acceleration produced

by the gravitational wave on test masses pairs. The acceleration is measured by modulating the frequency of the laser beam that travels from one test mass to the other. The initial LISA project, with a 5 Million km arm length, used a constellation of three spacecrafts containing the free falling test masses and flying as an equilateral triangle lagging the Earth by 20 degrees. NASA dropped support to the mission in 2011 for budget reasons and LISA was redesigned as an ESA mission. The choice of a shorter arm length and of a different orbit defined the new concept of eLISA, that has been selected by ESA for a L3 Science Theme, with a predicted launch scheduled in 2034 [9]. eLISA consists of three spacecrafts (the mother and two daughters) orbiting the Sun in nearly circular orbits and building an interferometer with one million km arm length. An arm is defined by two spacecrafts. The spacecrafts contain test masses in free fall and shielded from external disturbances; the spacecraft is centered on the test mass using a set of thrusters. The acceleration of the spacecraft relative to the test mass is measured in loco and subtracted.

The LISA Pathfinder is the precursor to the eLISA mission, the demonstrator of the instrument and of its technology [10], a small scale version of the eLISA arm, with two test masses (2 kg Au-Pt cubes) at a distance of 0.38 m. The Pathfinder has been launched in December 2015. The flight has demonstrated the feasibility of free-falling reference test masses in orbit, achieving a low noise, smaller than a factor 5 than the initial specifications [11]. The noise is close to the specifications of the original LISA design.

Space based interferometers have a sensitivity curve that is shaped as a U. The sub-mHz low frequency region is dominated by the acceleration noise, produced by residual forces that act on the test masses. The sensitivity in the high frequency region, above some tens mHz, is dominated by the shot noise of the laser. The instrumental noise is accompanied by the noise produced by an astrophysical background, the confusion noise of the unresolved population of galactic close binaries [49], [14].

Novae, as all cataclysmic variables, emit gravitational waves at twice the orbital frequency and corresponding harmonics. The contribution of the harmonics can safely be neglected, since the eccentricity will be negligible due to the circularization of the orbits during evolution. The gravitational wave strain of a binary system is given by [124]:

$$h = 8.7 \times 10^{-21} \left( \frac{\mu}{M_{\odot}} \right) \left( \frac{M}{M_{\odot}} \right)^{\frac{2}{3}} \left( \frac{100pc}{r} \right) \left( \frac{f}{10^{-3}Hz} \right)^{\frac{2}{3}} \quad (4.1)$$

where  $M = M_1 + M_2$ ,  $\mu = \frac{M_1 M_2}{M_1 + M_2}$ ,  $M_1, M_2$  are the masses of the primary and secondary star,  $r$  the cataclysmic distance and  $f$  the frequency.

The strain  $h$  is reported in Fig. 6 for the 156 cataclysmic variables investigated by [61], split into novae (full circles) and non novae cataclysmic variables (empty circles), data from [61]. The solid curve is the sensitivity of the LISA interferometer [8]. The dashed curve is the contribution of confusion noise <sup>6</sup>, the astrophysical background produced by unresolved binary systems [49], [14]. The instrumental noise and the confusion noise have been estimated for 1 year of integration time and unit signal to noise ratio.

Compared to other cataclysmic variables, novae are not the most promising sources for gravitational wave emission, due to their long orbital periods.

<sup>6</sup><http://www.srl.caltech.edu/shane/sensitivity/>

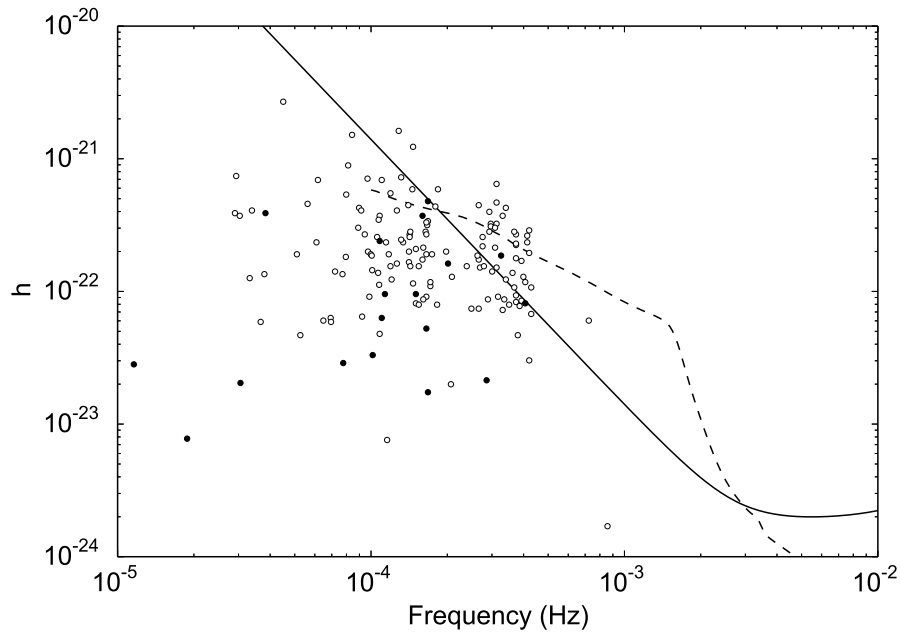


**Figure 6:** Gravitational wave emission of novae (full circles) and of non novae cataclysmic variables (empty circles), data from [61]; the solid curve is the instrumental sensitivity of the LISA interferometer, while the dashed line is the binary confusion noise, where both noise curves have been estimated assuming 1 year of integration time and unit signal to noise ratio

## 5. Conclusions

Novae are suitable multiwavelength laboratories to investigate the accretion process. A rich variety of physical processes are involved. Systematic investigation of novae at all wavelengths are required to address the problems of long term evolution and of the different populations in the Milky Way and in other galaxies.

## Acknowledgments

The author thanks the organizers for the invitation to the workshop. The author is grateful to the Department of Physics, University of Pisa and to Istituto Nazionale di Fisica Nucleare, Sezione di Pisa, for the travel support. Many thanks to the Telescope Allocation Time of the Loiano Observatory for the observing time. The author is grateful to the referee for the careful comments.

## References

- [1] B. P. Abbott et al., *PRL* **116** (2016a) 061102.
- [2] B. P. Abbott et al., *PRL* **116** (2016b) 241103.
- [3] A. A. Abdo et al., *Sci* **329** (2010) 817.
- [4] M. Ackermann et al., *Sci* **345** (2014) 554.

- [5] M. Actis et al., *ExA* **32** (2001) 143.
- [6] M. L. Ahnen et al., *A&A* **582** (2015) 582.
- [7] C. W. Allen, *MNRAS* **114** (1954) 387.
- [8] P. Amaro-Seoane et al., *CQG* **29** (2012) 124016.
- [9] P. Amaro-Seoane et al., *GW Notes* **6** (2013) 4.
- [10] F. Antonucci et al., *CQG* **29** (2012) 124014.
- [11] M. Armano et al., *PRL* **116** (2016) 231101.
- [12] H. C. Arp et al., *AJ* **61** (1956) 15.
- [13] W. B. Atwood et al., *ApJ* **697** (2009) 1071.
- [14] P. L. Bender and D. Hils, *CQG* **14** (1997) 1439.
- [15] M. F. Bode and A. Evans, *Classical Novae*, Cambridge University Press 2012.
- [16] Y. Cao et al., *ApJ* **752** (2012) 133.
- [17] M. Capaccioli et al., *AJ* **97** (1989) 1622.
- [18] M. Capaccioli et al., *ApJ* **360** (1990) 63.
- [19] A. Cassatella and R. Viotti, *Physics of Classical Novae*, Springer-Verlag, Lecture Notes in Physics 369 (1990).
- [20] C. C. Cheung et al., *ApJ* **826** (2016) 142.
- [21] R. Ciardullo et al., *ApJ* **356** (1990) 472.
- [22] D. D. Clayton and F. Hoyle, *ApJ* **187** (1974) 101.
- [23] J. G. Cohen, *ApJ* **292** (1985) 90.
- [24] A. C. Collazzi et al., *AJ* **138** (2009) 1846.
- [25] I. Czekala et al., *ApJ* **765** (2013) 57.
- [26] M. J. Darnley et al., *MNRAS* **369** (2006) 257.
- [27] M. J. Darnley et al., *ApJ* **833** (2016) 149.
- [28] G. de Vaucouleurs, *ApJ* **223** (1978) 351.
- [29] M. Della Valle, in: *The extragalactic distance scale*, *ASPC* **4** (1988) 73.
- [30] M. Della Valle et al., *A&A* **266** (1992) 232.
- [31] M. Della Valle et al., *A&A* **287** (1994) 403.
- [32] M. Della Valle, in *Classical Nova Explosions*, *AIPC* **637** (2002) 443.
- [33] M. della Valle and M. Livio, *A&A* **286** (1994) 786.
- [34] M. della Valle and M. Livio, *ApJ* **452** (1995) 704.
- [35] M. della Valle and M. Livio, *ApJ* **506** (1998) 818.
- [36] R. A. Downes and H. W. Duerbeck, *AJ* **120** (2000), 2007.
- [37] R. A. Downes et al., *JAD* **11** (2005) 2

- [38] H. W. Duerbeck, *SSR* **45** (1987) 1.
- [39] H. W. Duerbeck, *MNRAS* **258** (1992) 629.
- [40] H. W. Duerbeck, *AN* **330** (2009) 568.
- [41] A. Ederoclite, in: *Stella Novae: Past and Future Decades*, *ASPC* **490** (2014) 163.
- [42] F. Giovannelli and L. Sabau-Graziati, in Proceedings of *The Golden Age of Cataclysmic Variables and Related Objects - III*, *PoS (Golden2015)* 001 (2016).
- [43] J. A. Graham, in *Changing Trends in Variable Star Research*, *IAU Coll.* **46** (1979) 96.
- [44] I. Hachisu and M. Kato, *ApJSS* **167** (2006) 59.
- [45] I. Hachisu and M. Kato, *ApJ* **709** (2010) 680.
- [46] K. Hatano et al., *MNRAS* **290** (1997) 113.
- [47] N. Henze et al., *A&A* **582** (2015) 8.
- [48] M. Hernanz, in *Stella Novae: Past and Future Decades*, *ASPC* **490** (2014) 319.
- [49] D. Hils et al., *ApJ* **360** (1990) 65.
- [50] R. Hounsell et al., *ApJ* **734** (2010) 480.
- [51] R. Hounsell et al., *ApJ* **820** (2016) 104.
- [52] E. P. Hubble, *ApJ* **69** (1929) 103.
- [53] K. Imamura and K. Tanabe, *PASJ* **64** (2012) L9.
- [54] S. Kafka, these proceedings
- [55] M. M. Kasliwal et al., *ApJ* **735** (2011) 94.
- [56] M. Kato and I. Hachisu, *ApJ* **437** (1994) 803.
- [57] W. Liller and B. Mayer, *PASP* **99** (1987) 600.
- [58] LISA Study Team, 1998, in *LISA Pre-Phase A Report. 2nd Edition*, **Publication MPQ-233** (1998) Max-Planck Institute for Quantum Optics, Garching.
- [59] M. Livio, *ApJ* **393** (1992) 516.
- [60] F. Matteucci et al., *A&A* **405** (2003) 23.
- [61] M. T. Meliani et al., *A&A* **358** (2000) 417.
- [62] B. D. Metzger et al., *MNRAS* **450** (2015) 2739.
- [63] B. D. Metzger et al., *MNRAS* **457** (2016) 1786.
- [64] V. N. Mironovskii, *SvA* **9** (1966) 752.
- [65] P. Mroz et al., *ApJS* **219** (2015) 26.
- [66] P.Mroz et al., *ApJS* **232** (2016a) 9.
- [67] P. Mroz et al., *Nat* **537** (2016b) 649.
- [68] <https://asd.gsfc.nasa.gov/Koji.Mukai/novae/novae.html>
- [69] J. U. Ness, *BASI* **40** (2012) 353.



- [70] M. Orio, *RMxAA (Ser. Confer.)* **20** (2004) 182.
- [71] M. Orio, *BASI* **40** (2012) 333.
- [72] M. Orio, in Proceedings of *The Golden Age of Cataclysmic Variables and Related Objects - III*, *PoS (Golden2015) 064* (2016).
- [73] M. Orio, these proceedings
- [74] J. P. Osborne, *JHEAp* **7** (2015) 117.
- [75] A. Özdönmez et al., *MNRAS* **461** (2016) 1177.
- [76] A. Pagnotta, in *20th European White Dwarf Workshop, ASPC* **509** (2017) 535.
- [77] J. Patterson, *SASS* **33** (2014) 17.
- [78] C. H. Payne-Gaposchkin, *The Galactic Novae*, North-Holland Pub. Co. (1957).
- [79] W. Pietsch, *AN* **331** (2010) 187.
- [80] R. Poggiani, *AN* **327** (2006) 895.
- [81] R. Poggiani, *NewA* **13** (2008a) 557.
- [82] R. Poggiani, *Ap&SS* **315** (2008b) 79.
- [83] R. Poggiani, *NewA* **14** (2009a) 4.
- [84] R. Poggiani, *AN* **330** (2009b) 77.
- [85] R. Poggiani, *Ap&SS* **323** (2009c) 319.
- [86] R. Poggiani, *NewA* **15** (2010a) 657.
- [87] R. Poggiani, *NewA* **15** (2010b) 170.
- [88] R. Poggiani, *Ap&SS* **333** (2011) 115.
- [89] R. Poggiani, *MmSAI* **83** (2012) 753.
- [90] R. Poggiani, *NewA* **37** (2015) 9.
- [91] H. Ritter and U. Kolb, *A&A* **404** (2003) 301.
- [92] <http://wwwmpa.mpa-garching.mpg.de/RKcat/>
- [93] E. L. Robinson, *AJ* **80** (1975) 515.
- [94] L. Rosino, *AnAp* **27** (1964) 498.
- [95] L. Rosino, *A&AS* **9** (1973) 347.
- [96] L. Rosino, *AJ* **97** (1989) 83.
- [97] B. E. Schaefer, *ApJS* **187** (2010) 275.
- [98] T. Schmidt, *Z. Astrophys.* **41** (1957) 182.
- [99] G. J. Schwarz et al., *MNRAS* **320** (2001) 103.
- [100] A. W. Shafter, *ApJ* **487** (1997) 226.
- [101] A. W. Shafter, in: *Classical Nova Explosions: International Conference on Classical Nova Explosions, AIPC* **637** (2002) 462.

- [102] A. W. Shafter et al., *ApJ* **690** (2009) 1148
- [103] A. W. Shafter et al., *ApJ* **734** (2011) 12.
- [104] A. W. Shafter et al., *ApJ* **752** (2012) 156.
- [105] A. W. Shafter, *AJ* **145** (2013) 117.
- [106] A. W. Shafter, in: *Stella Novae: Past and Future Decades*, *ASPC* **490** (2014) 77.
- [107] A. W. Shafter et al., *ApJS* **216** (2015) 34.
- [108] A. W. Shafter, *ApJ* **834** (2017) 196.
- [109] A. W. Shafter and P. K. Irby, *ApJ* **563** (2001) 749.
- [110] M. M. Shara et al., *ApJ* **311** (1986) 163.
- [111] M. M. Shara et al., *Nat* **446** (2007) 159.
- [112] M. M. Shara et al., *ApJ* **758** (2012) 121.
- [113] M. M. Shara et al., *ApJSS* **227** (2016) 1.
- [114] M. M. Shara et al., *ApJ* **839** (2017) 109.
- [115] A. S. Sharov, *SvA* **16** (1972) 41.
- [116] A. S. Sharov, *AstL* **19** (1993) 147.
- [117] J. Sitarek and W. Bednarek, *PRD* **86** (2012) 063011.
- [118] J. L. Sokoloski, these proceedings
- [119] R. J. Strobe et al., *AJ* **140** (2010) 34.
- [120] F. Surina et al., arXiv:1111.5524 (2011).
- [121] J. Tanaka et al., *PASJ* **63** (2011) 911.
- [122] C. Tappert et al., *MNRAS* **423** (2012) 2476.
- [123] C. Tappert et al., in: Proceedings of *The Golden Age of Cataclysmic Variables and Related Objects - III*, *PoS (Golden2015)* **062** (2016).
- [124] K. S. Thorne, in *Three Hundreds Years of Gravitation* (1987) 330, Cambridge University Press, Cambridge, eds. S. Hawking and W. Israel.
- [125] A. B. Tomaney and A. W. Shafter, *ApJS* **81** (1992) 683.
- [126] S. van den Bergh, *PASP* **103** (1991) 609.
- [127] S. Vitale, *GRG* **46** (2014) 1730.
- [128] F. M. Walter et al., *PASP* **124** (2012) 1057.
- [129] F. M. Walter, in *Stella Novae: Past and Future Decades*, *ASPC* **490** (2014) 191.
- [130] R. E. Williams et al., *ApJ* **376** (1991) 721.
- [131] R. E. Williams, *AJ* **104** (1992) 725.
- [132] R. E. Williams et al., *ApJSS* **90** (1994) 297.
- [133] R. E. Williams, *JAD* **9** (2003).

- [134] R. E. Williams and A. W. Shafter, *ApJ* **612** (2004) 867.
- [135] R. Williams, *AJ* **144** (2012) 98.
- [136] O. Yaron et al., *ApJ* **623** (2005) 398.
- [137] L. Yungelson et al., *ApJ* **481** (1997) 127.